Nonlinear Multimodal Interference as Ultrafast Photonic Device for Dual-Wavelength Domain-Wall Dark Pulse Generation

Shan Wang(王珊), Bo-Le Song(宋博乐), Xin-He Dou(窦鑫河), Fei-Hong Qiao(乔飞鸿), Xiang Li(李响), Jin-Bo Wang(王锦波), and Zhi-Guo Lv(吕志国)*

School of Physical Science and Technology, Key Laboratory of Semiconductor Photovoltaic Technology of Inner Mongolia Autonomous Region, Inner Mongolia University, Hohhot 010021, China

(Received 5 April 2024; accepted manuscript online 13 June 2024)

In comparison to bright pulses, better stability that is not susceptible to loss makes dark pulses accessible for applications in such fields as signal processing, optics sensing, and quantum communication. Here we investigate the dual-wavelength domain-wall dark pulse generation in a graded-index multimode fiber (GIMF) based anomalous dispersion single-mode fiber (SMF) laser. By optimizing intra-cavity nonlinearity and pulse polarization, the mode-locked states can evolve each other between bright pulses, dark pulses, and bright-dark pulse pairs. The evolution mechanism among them may be relevant to the coherent mode superposition, spectral filtering, and mode selection in SMF-GIMF-SMF hybrid-fiber modulation devices that affect the pulse formation and evolution in temporal, frequency, and space domains. These results provide a valuable reference for promoting further development of nonlinear optics and ultrafast optics, in which ultrafast photonic devices, with low cost, simple manufacture as well as wide adaptability, as novel pulsed generation technique, play a vital role.

DOI: 10.1088/0256-307X/41/7/074203

In the last few years, graded-index multimode fibers (GIMFs) have become extensively studied subject due to their unique properties. New nonlinear dynamics such as Kerr self-cleaning,[1] nonlinear polarization dynamics,[2] supercontinuum generation,[3] and spatiotemporal mode-locking[4] have been investigated extensively. In addition to the aforementioned studies, nonlinear multimodal interference (NL-MMI) related saturable absorber behavior in GIMFs is theoretically proposed by Mafi *et al.* [5] Subsequently, numerous experimental investigations on NL-MMI based mode-locked lasers have been performed in different dispersion regimes.[6–14] On the other hand, due to the multimodal interactions in GIMFs, the phase difference between excitation modes will undergo periodic changes, resulting in coherent mode superposition and stable fundamental transverse mode generation.[15] In the meantime, the mode with the largest relative intensity can be maximally coupled into the following single-mode fiber (SMF), thus realizing the mode selection between GIMF and SMF.[16] Not only the incident light at different wavelengths for a fixed-length GIMF will have different transmittance in the GIMF-SMF composite fiber structure, but also the specific wavelengths of light can self-focus at the output position, thereby facilitating a good filtering effect in the laser and act as a wavelength filter.[17] In conclusion, the intricate interactions that occur within the SMF-GIMF-SMF composite fiber structure render it an optimal methodology for investigating the diverse nonlinear dynamics of pulses.

To date, various types of optical solitons have been experimentally generated in lasers based on NL-MMI, including dissipative soliton resonance, soliton molecules, noise-like pulses, and so on.[18–23] However, for the references listed above, all of them can be classified as bright solitons in some sense. In general, both bright and dark solitons could be generated in lasers and dictated by the energy distribution law. In the opposite of bright solitons, dark solitons are local pulses that appear as intensity dips on a continuous-wave background.[24] Furthermore, composite soliton states including bright-dark or dark-bright soliton pairs can also coexist in resonant cavity as results of interactions between solitons.[25–27] Dark pulses have exhibited extraordinary propagation properties and proven vast potential in signal processing, optics sensing, and quantum communication.[28–30] Consequently, further research is required to gain a deeper understanding of generation of dark pulses based on the NL-MMI mode-locking mechanism. This is an important area of research that has not been extensively investigated.

For several years, the generation technology on dark pulses has attracted widespread research interest in nonlinear optics and ultrafast optics fields.[31–33] According to its generation mechanism, dark pulses can be classified into nonlinear Schrödinger equation (NLSE) dark pulses, cubic-quintic nonlinear Schrödinger equation (CQNLSE) dark pulses, and domain wall (DW) dark pulses.[34–36] All of them exhibit similar characteristic in term of single dark pulse. However, there are significant differences in dispersion compensation as well as nonlinear management. Compared with that of the first two types, DW

*Corresponding author. Email: lvzhiguo@imu.edu.cn
© 2024 Chinese Physical Society and IOP Publishing Ltd

dark pulses do not depend on dispersion management or higher-order nonlinearity, but rather on the mutual interaction and coupling between two or more lasing in different wavelengths.[37,38] Most of the previous research work on dark pulse generation has utilized nonlinear polarization rotation and/or materials-based technique means.[39–43] Compared with the existing mode-locked technology, the ultra-fast photonic devices based on NL-MMI are simple, low-cost and pure optical fiber format, they also have the advantages of high damage threshold, wide bandwidth operation, and flexible parameter design. Thus, adopting the emerging SMF-GIMF-SMF hybrid-fiber modulation device to investigate DW dark soliton generation is yet to be studied. In the meantime, research on novel applications for emerging hybrid optical fiber modulator devices is of great significance to development of laser technology.

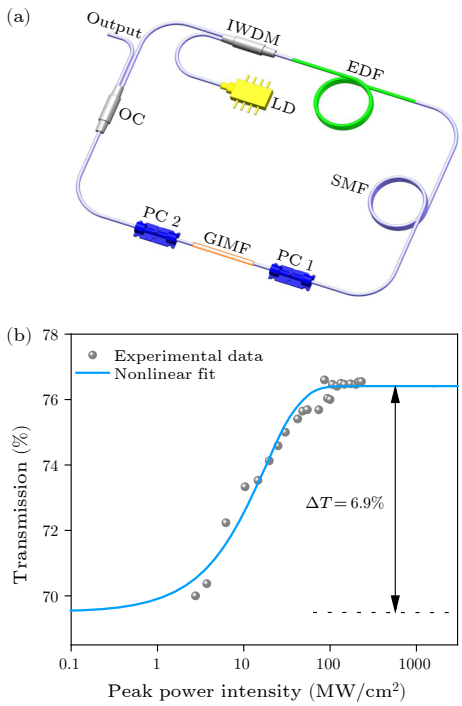

Fig. 1. (a) Experimental setup of dual-wavelength DW dark pulse laser with SMF-GIMF-SMF hybrid-fiber-based SA. LD: laser diode; IWDM: integrated device including polarization-independent isolator and wavelength division multiplexer; EDF: erbium-doped fiber; PC: polarization controller; OC: optical coupler. (b) Nonlinear optical transmission of the SMF-GIMF-SMF-based SA.

Herein, dual-wavelength DW dark pulses at 1567.95 and 1569.32 nm with signal-to-noise ratio (SNR) greater than 80 dB are generated in an anomalous dispersion laser based on the hybrid-fiber modulation device. Different from that reported in most of the references, herein without the aid of both polarization optics and nonlinear medium to introduce polarization-dependent loss and to enhance nonlinear effects, the generated dual-wavelength DW dark pulses depend entirely on strong coupling between two laser beams of different wavelengths and nonlinear evolution in the SMF-GIMF-SMF hybrid-fiber structure. Further, by carefully optimizing intra-cavity nonlinearity and pulse polarization, the pulsed states can evolve each other between bright pulses, bright-dark pulse pairs, and dark pulses. Research of multimode interference equivalent mode-locked devices used for dark soliton generation would be a promising field of optical solitons and has important research significance to realize both scheme innovation and performance breakthrough of pulsed laser generation.

Experimental Setup. Figure 1(a) presents the experiment scheme of the dual-wavelength DW dark pulse laser. In this cavity, a 60 cm section of Er-doped fiber (EDF, Liekki Er110-4/125) is used as the gain medium. Its peak core absorption is about 110 dB/m with a dispersion of 0.012 ps^2/m at 1550 nm. The 976 nm single-mode laser diode (LD) is coupled to the resonant cavity via an integrated hybrid device (IWDM) including polarization-independent isolator and 976/1550 nm wavelength division multiplexer. The polarization controllers (PCs) are used to manage the intra-cavity birefringence and NL-MMI effect. The hybrid-fiber (SMF-GIMF-SMF) structure utilized in our research work consists of a section of 90 cm GIMF (GI 62.5/125, Corning) sandwiched between two segments of SMF (SM28e, Corning), which acts as the ultrafast modulation device for pulsed laser generation. Next to the hybrid-fiber structure, a 10:90 optical coupler (OC) extracts ∼10% power from the cavity for mode-locked characteristics detection. The total length of the fiber cavity is 18.51 m, resulting in a net cavity dispersion of $-0.4\,ps^2$.

To achieve saturable absorption, the length of GIMF must satisfy $L = (n + 0.5)L_\pi$, where n is an odd integer and L_π is the self-imaging beat length.[44] In general, the fine-tuning range is small for SA purposes due to L_π in the micrometer range. To address the technical issue, approaches such as adding a section of SIMF or NCF, or introducing core-offset into the SMF-GIMF-SMF structure, have been taken to perform up to the required specification.[9,45–48] Conversely, the nonlinear optical transmittance of the hybrid-fiber (SMF-GIMF-SMF) structure can be influenced by bending the GIMF due to the variation in the ratio of high-order mode coupling into SMF. Thus, as the appropriate bending state is reached, the hybrid-fiber structure could act in temporal domain as an effective SA, and accomplish the spectral filter in frequency domain, which may be associated with the generation of dual-wavelength domain-wall (DW) dark pulses.

The nonlinear transmittance properties are measured using a home-made ultrafast fiber laser centered at 1570 nm with 92.25 MHz repetition rates, as shown in Fig. 1(b). The experimental values are fitted by the following formula:

$$T(I) = 1 - \Delta T \times \exp\Big(-\frac{I}{I_{\rm sat}}\Big) - \alpha_{\rm ns}, \qquad (1)$$

where $T(I)$ is the transmission, ΔT is the modulation depth, I is the input light intensity, $I_{\rm sat}$ is the saturation intensity, and $\alpha_{\rm ns}$ is the non-saturable loss. The calculated ΔT, $I_{\rm sat}$, and $\alpha_{\rm ns}$ are 6.9%, 17.25 MW/cm^2, and 23.6%, respectively.

Conventional Soliton Mode-Locking Operation. With the increment in pump power up to 214 mW, the laser achieves the stable conventional soliton mode-locked operation. The oscilloscope sequence in Fig. 2(a) shows that the interval between adjacent pulses is 92.57 ns, which aligns with the round-trip time of the ring cavity. The corresponding spectrum is presented in Fig. 2(b), which exhibits symmetrically distributed Kelly sidebands on both sides. Its central wavelength and 3 dB bandwidth are 1569.6 and 2.6 nm, respectively. As shown in Fig. 2(c), the autocorrelation trace shows a sech^2 intensity profile, which provides an estimation of the pulse duration to be 1.1 ps. The time-bandwidth product (TBP) is calculated to be 0.35, which is slightly larger than the Fourier transform limited value of 0.315. The pulse chirp may originate from the dispersion of the pigtail of the OC. The radio-frequency (RF) spectrum with 10 Hz resolution bandwidth is measured in order to determine whether the operation is single pulse. Figure 2(d) shows that the RF peak is centered at 10.803 MHz and the signal-to-noise ratio (SNR) is over 75 dB, indicating the excellent stability for fundamental mode-locked operation.

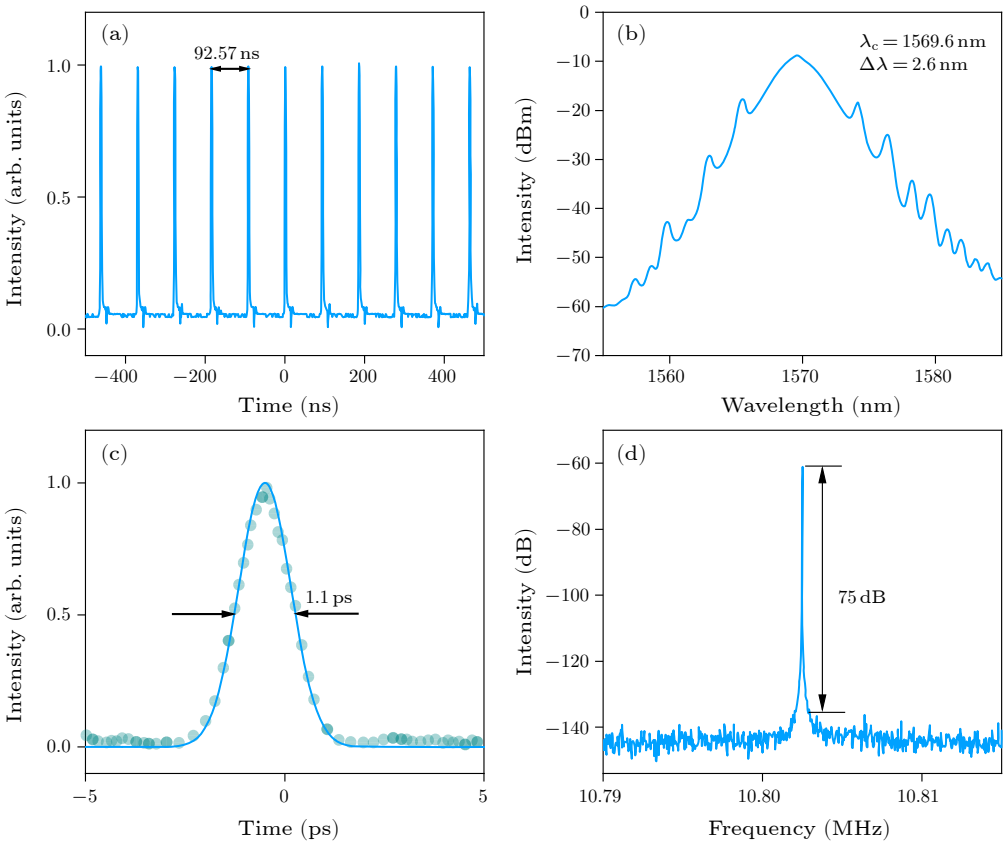

Fig. 2. Measured (a) pulse train, (b) optical spectrum, (c) autocorrelation trace, (d) RF spectrum at pump power of 214 mW.

Dual-Wavelength DW Dark Pulse Mode-Locking Operation. Further, by optimizing the pulse polarization and manipulating the laser gain, dual-wavelength dark pulses can be generated as the pump power is increased to 300 mW. Figure 3(a) shows that the interval between adjacent dark pulses is 92.57 ns, which aligns with the conventional soliton mode-locked operation. The corresponding spectra are shown in Fig. 3(b), with double peak emissions at 1567.95 and 1569.32 nm. In the case, Kelly sidebands are not observable. The generation mechanism is attributed to the propagation of the input optical field through the SMF-GIMF-SMF-based SA, where the four-wave mixing effect occurs as a result of the enhanced nonlinear effects. This effectively suppresses the mode competition that is typically observed in uniform broadening in the EDF gain medium, thus achieving the dual-wavelength mode-locked operation. The RF spectra are recorded for different frequency ranges. As shown in Fig. 3(c), the pulse repetition rate is centered at 10.803 MHz, and the SNR is better than 80 dB, indicating that the dual-wavelength dark pulse operates stably at the fundamental frequency. Furthermore, Fig. 3(d) depicts wider RF spectra with 200 MHz span, and no modulation is observed. This indicates that, despite the dual-wavelength coexistence in the cavity, only one resonant frequency is observed, which is representative of the characteristics of a dark pulse operation in a dual-wavelength system.[49] In addition, apart from the four-wave mixing effect, the generation of the dual-wavelength DW dark pulse is also relevant to the complex interactions in the SMF-GIMF-

SMF structure, such as spectral filtering, mode selection, and coherent mode superposition, which are all associated with the mutual coupling of the two wavelengths. The average output power is plotted against the launched pump power in Fig. 4(a). It can be seen that the maximum output power is 23.8 mW, which is limited by the available pump power. Additionally, a long-term power test in the dual-wavelength DW dark pulse mode-locked operation is conducted. As shown in Fig. 4(b), the power fluctuation measured over six hours is very small, with a root mean square (RMS) of 0.46%. These results confirm the reliable operation of the dual-wavelength DW dark pulse mode-locking state, making it a promising candidate in such fields as signal processing, optics sensing, and quantum communication.

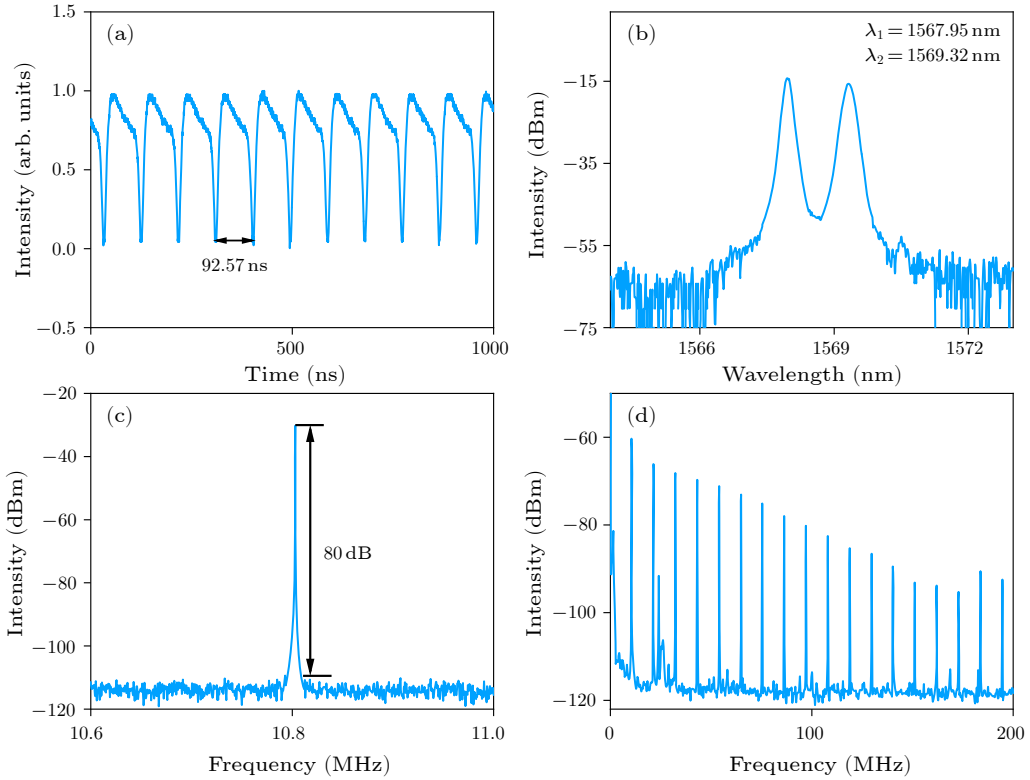

Fig. 3. Characteristics of dual-wavelength DW dark pulses: (a) pulse train, (b) optical spectrum, (c) RF spectrum, (d) RF spectrum within the 0–200 MHz range.

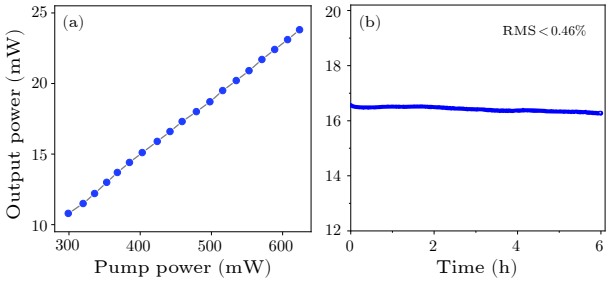

Fig. 4. (a) The average output power versus the pump power. (b) Power stability of the laser for 6 hours.

Evolution of Bright-Dark Pulse Pairs. Interestingly, by changing the pumping power, pulse polarization, and other parameters, another fascinating soliton formation and evolution are observed. It can be demonstrated that the transition from bright-dark soliton pairs to dark-bright soliton pairs is possible. As shown in Fig. 5(a), in polarization state 1, the bright and dark pulses are entangled with each other to form the tightly bound bright-dark soliton pairs. Then, the dark pulse starts to move away from the bright pulse as the rotation angle of the PC changes. This phenomenon may be due to the weakened interaction between them. Furthermore, as the polarization angle increases to polarization state 4, the dark pulses can be entangled with the latter bright pulses once again, which can be equivalent to generating dark-bright soliton pairs. In addition, as the orientation of PCs returns to initial polarization state 1, the bright-dark soliton pairs can be generated again. As shown in Fig. 5(b), the dual-wavelength DW mode-locked spectra also change during the evolution of the mode-locked state. This phenomenon proves that the SMF-GIMF-SMF hybrid fiber structure has not only the saturable absorption effect, but also the birefringence-induced filtering effect as mentioned above. By rotating the PCs, the transmission performance (central wavelength, bandwidth) of the band-pass filter bases on multimode interference in the SMF-GIMF-SMF hybrid fiber structure can be changed accordingly. Thus, both the transmitted spectral shape and wavelength spacing

can be changed. In addition, the change in birefringence induced by the applied strain causes a relative propagation delay between the bright and dark pulses, but both of them could still bound together and propagate at the same velocity. Therefore, the change in dual-wavelength DW mode-locked spectra will result in a tunable pulse envelope.

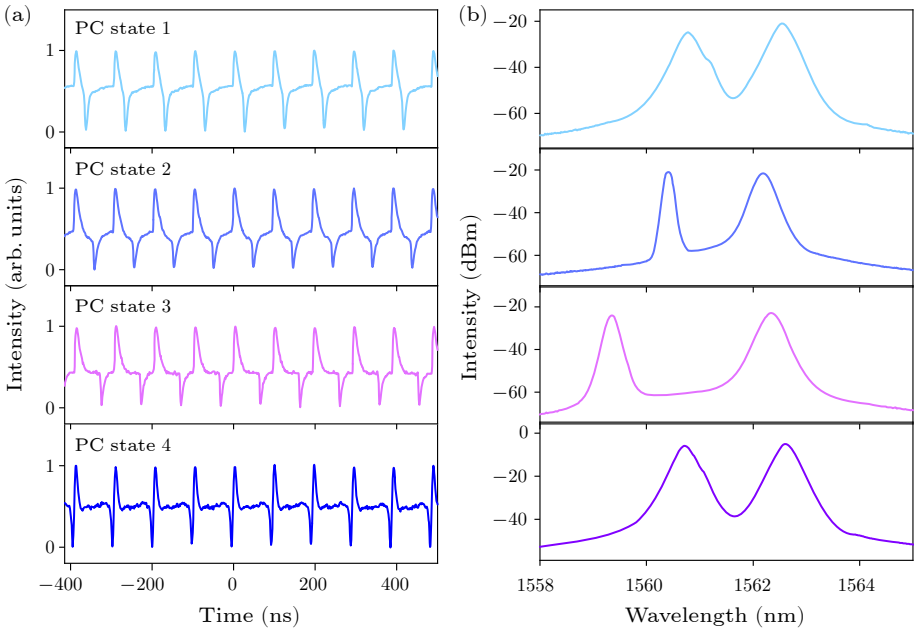

Fig. 5. (a) Pulse train, and (b) optical spectra evolution process during the transition from bright-dark soliton pairs to dark-bright soliton pairs.

In conclusion, we report experimental research on the generation of dual-wavelength DW dark pulses in an anomalous dispersion laser by adopting SMF-GIMF-SMF structure as an ultrafast photonic mode-locked device. The dual-wavelength DW dark pulse mode-locked operation is centered at 10.803 MHz, and the SNR is better than 80 dB. Moreover, the mode-locked states can evolve mutually between bright pulses, dark pulses and bright-dark pulse pairs by optimizing intracavity nonlinearity and pulse polarization. These results confirm that the composite fiber structure is a promising modulation device for generating various types of the dual-wavelength DW dark pulses, and has important research significance to realize both scheme innovation and performance breakthrough of pulsed laser generation.

Acknowledgements. This work was supported by the National Natural Science Foundation of China (Grant No. 12164030), the Young Science and Technology Talents of Inner Mongolia (Grant No. NJYT22101), and the Central Government Guides Local Science and Technology Development Fund Projects (Grant No. 2023ZY0005).

References

[1] Liu Z, Wright L G, Christodoulides D N, and Wise F W 2016 *Opt. Lett.* **41** 3675
[2] Krupa K, Garmendia Castañeda G, Tonello A, Niang A, Kharenko D S, Fabert M, Couderc V, Millot G, Minoni U, Modotto D, and Wabnitz S 2019 *Opt. Lett.* **44** 171
[3] Krupa K, Louot C, Couderc V, Fabert M, Guenard R, Shalaby B M, Tonello A, Pagnoux D, Leproux P, Bendahmane A, Dupiol R, Millot G, and Wabnitz S 2016 *Opt. Lett.* **41** 5785
[4] Wright L G, Christodoulides D N, and Wise F W 2017 *Science* **358** 94
[5] Nazemosadat E and Mafi A 2013 *J. Opt. Soc. Am. B* **30** 1357
[6] Nazemosadat E and Mafi A 2013 *Opt. Express* **21** 30739
[7] Wang S, Lv Z, and Qiu J 2023 *Nanomaterials* **13** 535
[8] Wang H Y, Xiao Y J, Liu Q, Xing X W, Yang H J, and Liu W J 2023 *Chin. Phys. Lett.* **40** 114204
[9] Dong Z, Li S, Chen R, Li H, Gu C, Yao P, and Xu L 2019 *Opt. Laser Technol.* **119** 105576
[10] Wang Z K, Wang D N, Yang F, Li L J, Zhao C L, Xu B, Jin S Z, Cao S Y, and Fang Z J 2017 *J. Lightwave Technol.* **35** 5280
[11] Li X, Huang X, Han Y *et al.* 2023 *Ultrafast Sci.* **3** 0006
[12] Xiao Y J, Xing X W, Cui W W, Chen Y Q, Zhou Q, and Liu W J 2023 *Chin. Phys. Lett.* **40** 054201
[13] Li X, Huang X, Hu X, Guo X, and Han Y 2023 *Opt. Laser Technol.* **158** 108898
[14] Jiang H, Li H, Hu F, Ren X, Li C, and Xu S 2020 *IEEE Photon. Technol. Lett.* **32** 503
[15] Fabert M, Săpântan M, Krupa K, Tonello A, Leventoux Y, Février S, Mansuryan T, Niang A, Wetzel B, Millot G, Wabnitz S, and Couderc V 2020 *Sci. Rep.* **10** 20481
[16] Mafi A, Hofmann P, Salvin C J, and Schülzgen A 2011 *Opt. Lett.* **36** 3596
[17] Antonio-Lopez J E, Castillo-Guzman A, May-Arrioja D A, Selvas-Aguilar R, and LiKamWa P 2010 *Opt. Lett.* **35** 324
[18] Dong Z, Lin J, Li H, Li S, Tao R, Gu C, Yao P, and Xu L 2019 *Opt. Express* **27** 27610
[19] Cui W W, Xing X W, Chen Y Q, Xiao Y J, Ye H, and Liu W J 2023 *Chin. Phys. Lett.* **40** 024201
[20] Lv Z, Yang Z, Song D, Li F, Yang Y, Yang X, Wang Y, Li Q, and Zhao W 2019 *Opt. Laser Technol.* **119** 105626
[21] Zhang X, Yi H, Yao Y, Wang S, and Shi L 2023 *Chin. Phys. Lett.* **40** 124204

[22] Lv Z, Yang Z, Song D, Li F, Yang X, Yang Y, Wang Y, Li Q, and Zhao W 2019 *Appl. Phys. Express* **12** 022004
[23] Meng X C, Li L, Sun N Z, Xue Z, Liu Q, Ye H, and Liu W J 2023 *Chin. Phys. Lett.* **40** 124202
[24] Tang D, Guo J, Song Y, Zhang H, Zhao L, and Shen D 2014 *Opt. Express* **22** 19831
[25] Radhakrishnan R and Aravinthan K 2007 *J. Phys. A* **40** 13023
[26] Ning Q Y, Wang S K, Luo A P, Lin Z B, Luo Z C, and Xu W C 2012 *IEEE Photon. J.* **4** 1647
[27] Li X, Zhang S, Meng Y, and Hao Y 2013 *Opt. Express* **21** 8409
[28] Krökel D, Halas N J, Giuliani G, and Grischkowsky D 1988 *Phys. Rev. Lett.* **60** 29
[29] Baronio F, Frisquet B, Chen S, Millot G, Wabnitz S, and Kibler B 2018 *Phys. Rev. A* **97** 013852
[30] Zhang W, Zhan L, Xian T, and Gao L 2019 *Opt. Lett.* **44** 4008
[31] Du Y, Han M, and Shu X 2020 *Opt. Lett.* **45** 666
[32] Shen J, Huang X, Jiang S, Jiang R, Wang H, Lu P, Xu S, and Jiao M 2022 *Chin. Phys. Lett.* **39** 104201
[33] Song Y, Shi X, Wu C, Tang D, and Zhang H 2019 *Appl. Phys. Rev.* **6** 021313
[34] Tang D Y, Li L, Song Y F, Zhao L M, Zhang H, and Shen D Y 2013 *Phys. Rev. A* **88** 013849
[35] Tiu Z C, Suthaskumar M, Zarei A, Tan S J, Ahmad H, and Harun S W 2015 *Opt. Laser Technol.* **73** 127
[36] Zhang H, Tang D Y, Zhao L M, and Knize R J 2010 *Opt. Express* **18** 4428
[37] Zhang H, Tang D, Zhao L, and Wu X 2011 *Opt. Express* **19** 3525
[38] Wang P, Zhao K, Xiao X, and Yang C 2017 *Opt. Express* **25** 30708
[39] Gao J, Hu F M, Huo X D, and Gao P 2014 *Laser Phys.* **24** 085104
[40] Zhao R, Li G, Zhang B, and He J 2018 *Opt. Express* **26** 5819
[41] Huang K W, Wang X, Qiu Q Y, Wu L, and Xiong H 2023 *Chin. Phys. Lett.* **40** 104201
[42] Zhang W Y, Zhan L, Xian T H, and Gao L R 2019 *J. Lightwave Technol.* **37** 3756
[43] Lang Y, Peng Z, and Zhao Z 2022 *Chin. Phys. Lett.* **39** 114201
[44] Li H, Wang Z, Li C, Tian Y, Xiao Z, Zhang J, and Xu S 2019 *Opt. Laser Technol.* **113** 317
[45] Li H, Wang Z, Li C, Zhang J, and Xu S 2017 *Opt. Express* **25** 26546
[46] Li X, Huang X, Chen E, Zhou Y, and Han Y 2022 *Opt. Laser Technol.* **156** 108592
[47] Chang S, Wang Z K, Wang D N, Wu W D, and Gao F 2021 *Opt. Commun.* **483** 126612
[48] Pan W, Jin L, Wang J Z, Wang R Y, Zhang H, Yingtian X, Zhao X, Li Y, and Ma X H 2021 *Appl. Opt.* **60** 923
[49] Yang S, Zhang Q Y, Zhu Z W, Qi Y Y, Yin P, Ge Y Q, Li L, Jin L, Zhang L, and Zhang H 2022 *Opt. Laser Technol.* **152** 108116